EPJ Web of Conferences **137**, 07010 (2017) DOI: 10.1051/epjconf/201713707010
XIIth Quark Confinement & the Hadron Spectrum

Geometrical clusterization and deconfinement phase transition in SU(2) gluodynamics

A. Ivanytskyi[1,a], K. Bugaev[1,b], E.Nikonov[2], E.-M. Ilgenfritz[3], D. Oliinychenko[4], V. Sagun[1], I. Mishustin[4], G. Zinovjev[1], and V. Petrov[1]

[1] *Bogolyubov Institute for Theoretical Physics, 03680 Kyiv, Ukraine*
[2] *Laboratory for Information Technologies, JINR, 141980 Dubna, Russia*
[3] *Bogolyubov Laboratory of Theoretical Physics, JINR, 141980 Dubna, Russia*
[4] *FIAS, Goethe University, Ruth-Moufang Str. 1, 60438 Frankfurt upon Main, Germany*

Abstract. A novel approach to identify the geometrical (anti)clusters formed by the Polyakov loops of the same sign and to study their properties in the lattice SU(2) gluodynamics is developed. The (anti)cluster size distributions are analyzed for the lattice coupling constant $\beta \in [2.3115, 3]$. The found distributions are similar to the ones existing in 2- and 3-dimensional Ising systems. Using the suggested approach, we explain the phase transition in SU(2) gluodynamics at $\beta = 2.52$ as a transition between two liquids during which one of the liquid droplets (the largest cluster of a certain Polyakov loop sign) experiences a condensation, while another droplet (the next to the largest cluster of opposite Polyakov loop sign) evaporates. The clusters of smaller sizes form two accompanying gases, which behave oppositely to their liquids. The liquid drop formula is used to analyze the distributions of the gas (anti)clusters and to determine their bulk, surface and topological parts of free energy. Surprisingly, even the monomer multiplicities are reproduced with high quality within such an approach. The behavior of surface tension of gaseous (anti)clusters is studied. It is shown that this quantity can serve as an order parameter of the deconfinement phase transition in SU(2) gluodynamics. Moreover, the critical exponent β of surface tension coefficient of gaseous clusters is found in the upper vicinity of critical temperature. Its value coincides with the one found for 3-dimensional Ising model within error bars. The Fisher topological exponent τ of (anti)clusters is found to have the same value 1.806 ± 0.008, which agrees with an exactly solvable model of the nuclear liquid-gas phase transition and disagrees with the Fisher droplet model, which may evidence for the fact that the SU(2) gluodynamics and the model are in the same universality class.

1 Introduction

Transition between the confined and deconfined states of strongly interacting matter in quantum chromodynamics (QCD) is one of the hot topics of modern theoretical physics. An exceptional difficulty of this non-abelian gauge theory makes impossible a study of the deconfinement phase transition (PT)

[a] e-mail: aivanytskyi@bitp.kiev.ua
[b] e-mail: bugaev@th.physik.uni-frankfurt.de

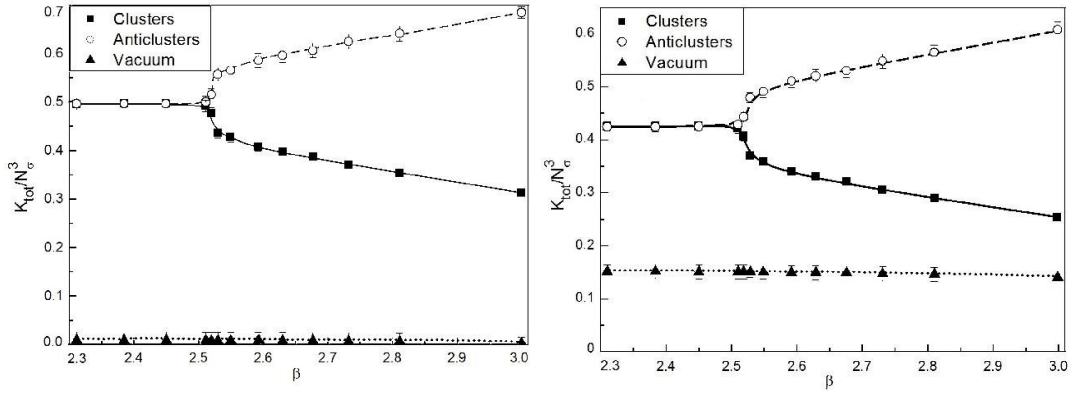

Figure 1. Total volume fraction of clusters, anticlusters and auxiliary vacuum measured for $L_{cut} = 0.1$ (left panel) and $L_{cut} = 0.2$ (right panel). The volume fraction of an auxiliary vacuum is independent on the Polyakov loop cut off. The curves are shown to guide the eye.

from first principles. However, numerical simulations on a discrete space-time lattice allow one to avoid some difficulties of QCD and to investigate its phase structure. On the other hand, the pure gauge non-abelian theory known as gluodynamics includes main features of the deconfinement PT and at the same time is much simpler than the full QCD with quarks. Moreover, the Svetitsky-Jaffe hypothesis [1, 2] establishes a correspondence between the PTs in d+1 dimensional SU(N) gluodynamics and Z(2) symmetric spin system in d dimensions. The role of the continuous gauge spin in gluodynamics is played by the Polyakov loop. The geometrical clusterization phenomenon is a well known feature of spin systems, which is responsible for a percolation. A similar phenomenon was also observed in pure gauge theories [3, 4]. Moreover, the vicinity of deconfinement PT in SU(2) gluodynamics was already studied within the percolation framework [5, 6], which was mainly concentrated on the properties of largest cluster. However, after invention of the Fisher Droplet Model [7, 8] and its successors it became clear that many features of PT are encoded in the properties of smaller clusters which were not studied within the percolation approach [5, 6]. Therefore, in this work we pay a special attention to the properties of small geometrical clusters in SU(2) gluodynamics. Using our novel approach we explain the transition between the confined and deconfined phases of gluodynamics as a special kind of the liquid-gas PT [9].

The work is organized as follows. Section 2 is devoted to the formal definitions of Polyakov loops and their geometrical (anti)clusters. In Section 3 the size distributions of geometrical (anti)clusters along with their fit with the liquid droplet formula are discussed. A special attention to fit of the monomers is payed in Section 4. The new order parameters are discussed in Section 5, while our conclusions are summarized in Section 6.

2 The Polyakov loop geometrical clusters

Let us remind that the local Polyakov loop $L(\vec{x})$ is defined at any spacial point $\vec{x}$ of (d+1)-dimensional lattice of size $N_\sigma^d \times N_\tau$. In terms of the temporal gauge links $U_4(\vec{x}, t)$ the definition of $L(\vec{x})$ is as follows

$$L(\vec{x}) = Tr \prod_{t=0}^{N_\tau - 1} U_4(\vec{x}, t). \tag{1}$$

SU(2) gauge group leads to the real values of Polyakov loop which belong to the interval $[-1; 1]$. This property of $L(\vec{x})$ allowed us to formulate a clear definition of geometrical clusters being a group of the

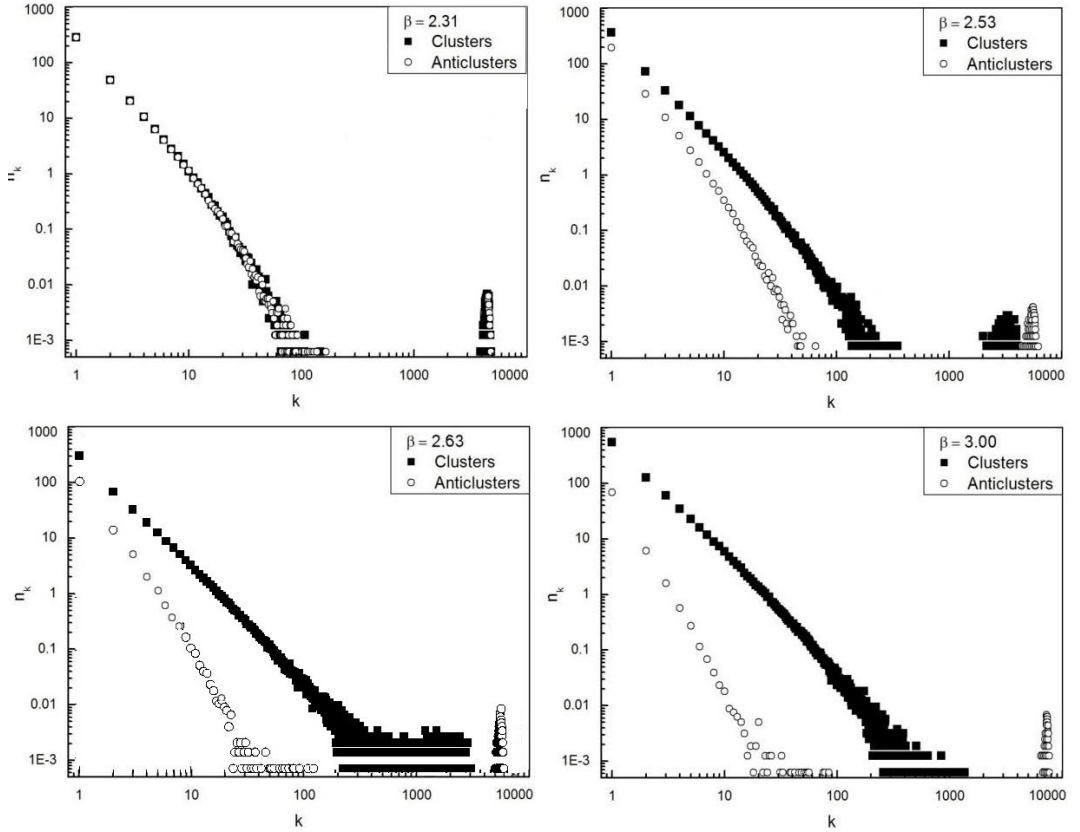

Figure 2. Size distributions of clusters (squares) and anticlusters (circles) for $\beta = 2.31$ (left upper panel), $\beta = 2.53$ (right upper panel), $\beta = 2.63$ (left lower panel) and $\beta = 3.0$ (right lower panel) are shown for the cut off $L_{cut} = 0.2$.

nearest neighboring lattice sites with the same sign of Polyakov loop. The strong fluctuations of this quantity on the boundaries of neighboring clusters which have the opposite signs of the Polyakov loop can be excluded from the consideration by introducing the minimal absolute value of the Polyakov loop attributed to the clusters [5, 6], i.e. by a cut off parameter $L_{cut} > 0$. If $|L(\vec{x})| \leq L_{cut}$ then the spacial point $\vec{x}$ is attributed to an "auxiliary" or "confining" vacuum. It is remarkable that the volume fraction of vacuum is independent of the lattice parameter $\beta = \frac{4}{g^2}$ (see Fig. 1) defined by the coupling constant g. Based on this definition we treat the monomers, the dimers, etc. as the clusters made of a corresponding number of "gauge spins" of the same sing which are surrounded either by the clusters of the opposite "spin" sign or by a vacuum [9]. In case of SU(2) group there are clusters of two types which differ by sign of the local Polyakov loop. According to our formal definition the anticlusters are made of the gauge spins of a sign which coincides with that one of the largest n-mer existing at a given lattice configuration. This largest anticluster is called the "anticluster droplet". It is accompanied by other n-mers of the same sign called as the "gas of anticlusters". For the same lattice configuration the similar objects which have an opposite sign of Polyakov loop are called as clusters and, hence, the largest of them is the "cluster droplet".

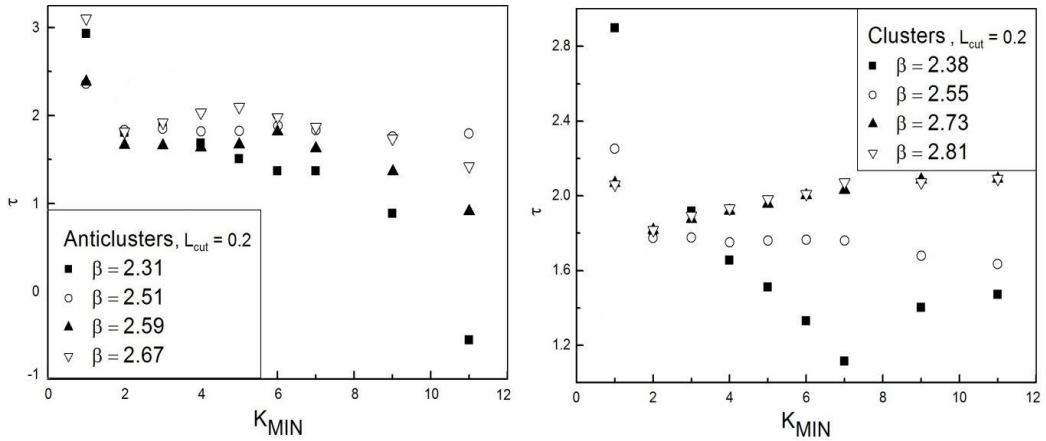

Figure 3. The Fisher exponent τ for several values of k_{min} and for a few values of β found by the 4-parametric fit of the LDM formula. All these results refer to the cut-off $L_{cut} = 0.2$.

3 Size distributions of clusters

In order to realize the described scheme of the (anti)cluster identification we performed the numerical simulations on the 3+1 dimensional lattice of the size $N_\sigma^d \times N_\tau = 24^d \times 8$ for 13 values of the lattice parameter β from 2.31 to 3. Concentration of β-points in the PT region is caused by its principal interest for this study. Two-loop β dependence of the lattice spacing $a(\beta)$ allows us to find the physical temperature as $1/T = N_\tau a(\beta)$ [5]. In this study we used two values of the Polyakov loop cut off $L_{cut} = 0.1$ and 0.2.

For each value of β the cluster size distributions were averaged over the ensemble of independent lattice configurations. For averaging we used several number of independent lattice configurations. If the averaged distributions found for different numbers of configurations were identical within statistical errors, then we used the results found for an ensemble of a largest number of configurations as the high statistics limit. This scheme allowed us to exclude the effects of strong statistical fluctuations. For almost all β values the results obtained for 800 and 1600 configurations were indistinguishable. However, in case of gaseous anticlusters at three largest values of β we used 2400 configurations, since in this case the statistics was rather poor. The right hand side vicinity of PT was also analyzed with higher statistics due to a principal interest to this region.

The typical size distributions of (anti)clusters n_k for $L_{cut} = 0.2$ are shown in Fig. 2. The global Z(2) symmetry exists at the lattice constant values below the critical value $\beta_c^\infty = 2.5115$ in an infinite system [10]. The (anti)cluster distributions are identical in this case (see the left upper panel of Fig. 2). If β is even slightly above β_c^∞ then the symmetry between (anti)clusters breaks down (see the right upper panel of Fig. 2). In this case the size of the cluster (anticluster) droplet decreases (increases). It is remarkable, that the corresponding gaseous clusters behave contrary to their droplets. Therefore, the deconfinement PT in SU(2) gluodynamics can be considered as an evaporation of the cluster droplet into the gas of clusters and a simultaneous condensation of the gas of anticlusters on the anticluster droplet. At high β (the lower panel of Fig. 2) the cluster droplet becomes indistinguishable from its gas, whereas the size of anticluster droplet becomes comparable to the size of system. From Fig. 2 one can see that the gas and liquid branches of anticluster distributions are well separated from each other. A similar behavior is seen for the clusters, except for high values of β, at which the cluster droplet simply disappears due to evaporation (see the lower panel of Fig. 2).

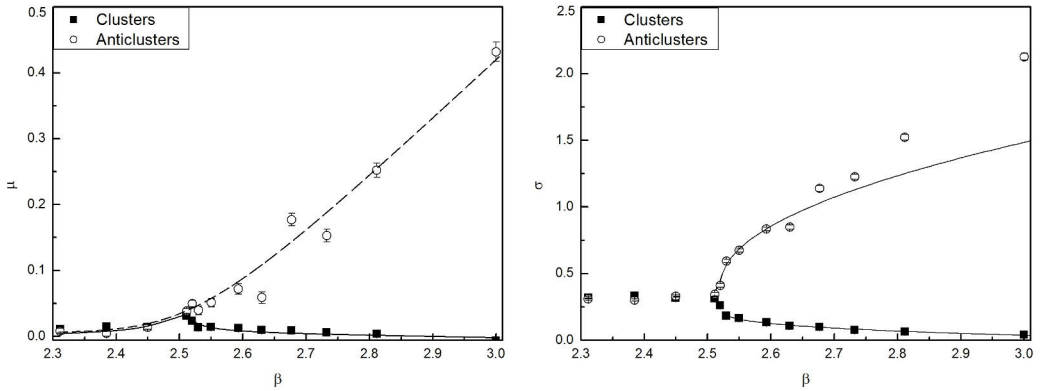

Figure 4. Reduced chemical potential μ_A (left panel) and the reduced surface tension σ_A (right panel) found from three parametric fit at $L_{cut} = 0.2$. The curves shown in the right panel represent Eq. (6).

The found distributions closely resemble the ones discussed for the nuclear fragments [11] and for the Ising spin clusters [12]. Hence, we analyzed whether the Liquid Droplet Formula (LDF) [7]

$$n_A^{th}(k) = C_A \exp\left(\mu_A k - \sigma_A k^{2/3} - \tau \ln k\right) , \tag{2}$$

is able to reproduce the size distributions of clusters ($A = cl$) and anticlusters ($A = acl$). Here $T\mu_A k$ and $T\sigma_A k^{2/3}$ denote, respectively, the bulk and the surface parts of free energy of k-mer (anti)cluster with the surface proportional to $k^{2/3}$, whereas τ denotes the Fisher topological constant, and C_A is the normalization factor. We found these parameters from the fit of the (anti)cluster size distributions, which also allowed us to determine the minimal size k_{min} to which the LDF can be applied. In practice, we minimized the quantity

$$\chi^2/dof = \frac{1}{k_{max} - k_{min} - n_{par}} \sum_{k=k_{min}}^{k_{max}} \left(\frac{n_A^{th}(k) - n_A(k)}{\delta n_A(k)} \right)^2 , \tag{3}$$

with respect to C_A, μ_A, σ_A, τ and k_{min}. Here k_{max} is the maximal size of the gaseous (anti)cluster, $\delta n_A(k)$ is the error of simulated $n_A(k)$ and n_{par} is the number of fitted parameters. This procedure was performed with the iterative gradient search method, in which the next approximation of the parameter vector $\vec{p}_A = (C, \mu, \sigma, \tau)_A$ is defined as

$$\vec{p}_A \to \vec{p}_A - \epsilon \cdot \vec{\nabla}_{\vec{p}_A} \chi^2/dof , \tag{4}$$

while the positive valued elements of the matrix $\epsilon = diag(\epsilon_C, \epsilon_\mu, \epsilon_\sigma, \epsilon_\tau)$ are used in order to optimize the fit procedure. This iterative scheme corresponds to a numerical solution of the equation $\vec{\nabla}_{\vec{p}_A} \chi^2/dof = 0$ which is a criterion of χ^2/dof minimization. We found that $\chi^2/dof \approx 1$ for all $k_{min} \geq 2$, whereas for $k_{min} = 1$ we got $\chi^2/dof \approx 10$, which corresponds to the low quality of data description. Hence, we are able to conclude that the LDF is already able to describe the dimers. Another argument in favor of $k_{min} = 2$ is related to the fact that for this value of k_{min} the Fisher topological constant is independent on β (see Fig. 3). This remarkable result is in line with framework of the statistical cluster models [7, 8, 11]. Thus, a four parametric fit ($n_{par} = 4$) of the LDF yields $k_{min} = 2$ and $\tau = 1.806 \pm 0.008$ both for clusters and for anticlusters. It is necessary to stress that the found value of τ agrees with the exactly solvable model of the nuclear liquid-gas PT [11] which has a tricritical

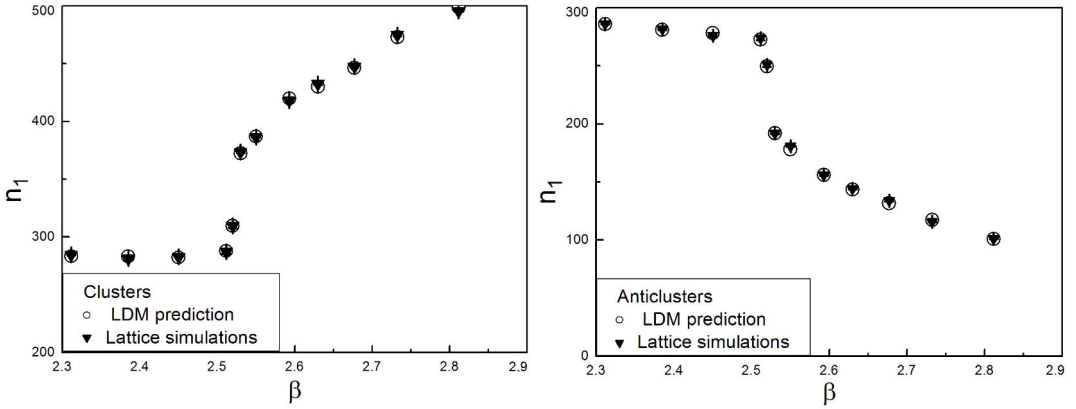

Figure 5. Monomer multiplicities of clusters (left panel) and anticlusters (right panel) for $L_{cut} = 0.2$.

endpoint, but it contradicts to the FDM [7, 8] which has a critical endpoint. Fixing the values of τ and k_{min} we could perform a three parametric fit ($n_{par} = 3$) of the (anti)cluster size distributions to define C_A, μ_A and σ_A with higher precision and less time for simulations. The typical value of $\chi^2/dof \approx 1$ was obtained for any β, which signals about the high quality of data description. The dependences of μ_A and σ_A on β are shown in Fig. 4 for $L_{cut} = 0.2$. For $L_{cut} = 0.1$ the results are qualitatively the same.

4 Properties of monomers

Although the monomers are the most abundant (anti)clusters in the gas, their description based on the formula (2) is rather poor. In order to analyze the behavior of the monomer multiplicities we used the following ansatz

$$n_A^{th}(1) = C_A g_A \exp(\mu_A V_1 - \sigma_A S_1), \tag{5}$$

where V_A and S_A are their effective volume and effective surface measured in the lattice units, respectively. These quantities are conjugated to the reduced chemical potential μ_A and the reduced surface tension coefficient σ_A taken from the fit of size distributions of (anti)cluster with the size $k \geq 2$. The parameter g_A accounts for a possible deviation of monomers from the abundances of other k-mers described by the normalization factor C_A. Treating V_A, S_A and g_A as the fitting parameters to be independent of β, it was possible to describe the monomers within the modified LDF (5), which proves a generality of the suggested approach.

Here we report the results of independent fits of the (anti)monomer multiplicities for $L_{cut} = 0.2$ (see Fig. 5). The point $\beta = 3$ was excluded from the analysis in order to eliminate the effects of strong numerical fluctuation caused by the low statistics of antimonomers. From Fig. 5 one can see that both the cluster and the anticluster multiplicities are well reproduced for all values of β analyzed here. At the same time somewhat large values of $\chi^2/dof = 7.12$ for clusters and $\chi^2/dof = 8.83$ for anticlusters are caused by exceptionally small errors of the monomer multiplicities. The obtained values of $V_{cl} = 0.9902$, $S_{cl} = 0.5251$, $g_{cl} = 1.1920$ and $V_{acl} = 0.2736$, $S_{acl} = 0.8462$, $g_{acl} = 1.3460$ demonstrate that the monomers, indeed, deviate form all other clusters, which justifies the modification of the LDF for them.

5 Order parameters of the deconfinement phase transition

A drastic change of the reduced surface tension coefficient behavior at the deconfinement PT is an important finding of this study. As one can see from the right panel of Fig. 4 for $\beta \leq \beta_c$ this quantity

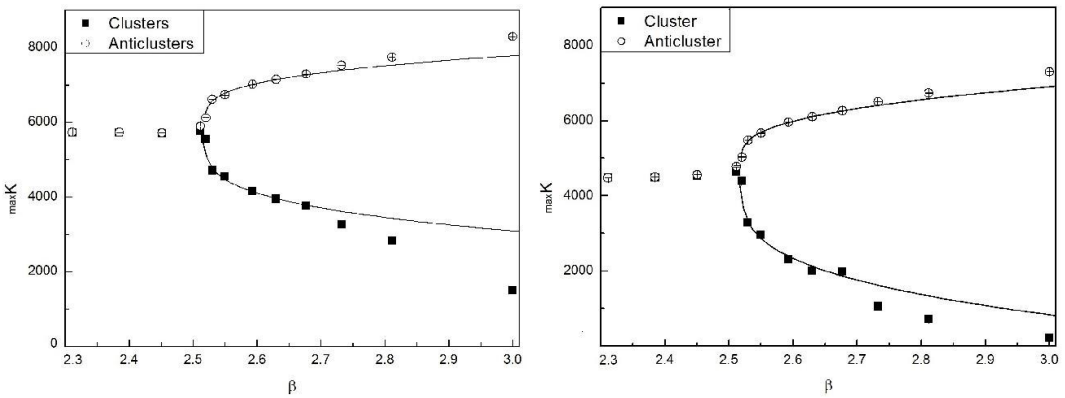

Figure 6. The mean size of the maximal (anti)cluster found for $L_{cut} = 0.1$ (left panel) and for $L_{cut} = 0.2$ (right panel). The curves represent Eq. (8).

is constant and it is identical for clusters and anticlusters. At the same time even a slight increase of β compared to its critical value $\beta_c = 2.52$ leads to a splitting of σ_A values for the clusters of different types. Indeed, for $\beta > \beta_c$ the surface tension coefficient of cluster σ_{cl} monotonically decreases, while the one of anticlusters σ_{acl} monotonically increases with β. This qualitative difference in the β-dependence of the reduced surface tension coefficient allows us to treat it as an order parameter of the deconfinement PT in SU(2) gluodynamics. Since the order parameter behavior is of principal interest for the theory of PT, then we analyzed the β-dependence of the reduced surface tension in the right hand side vicinity of β_c using the formula

$$\sigma_A(\beta) = \sigma_A(\beta_c) \pm d_A(\beta - \beta_c)^{B_A}. \tag{6}$$

Here d_A and B_A are the constants, while the signs "+" and "-" correspond to A = acl and A = cl, respectively. Eq. (6) fits σ_A with a high quality. The results of fit are given in Table 1. It is notable that despite the different values of d_A found for different cut offs, the exponents B_A weakly depend on L_{cut}.

The average value of Polyakov loop $\langle L(\vec{x})\rangle$ is traditionally considered as an order parameter of a PT in SU(2) gluodynamics. In [9] we showed that it is mainly defined by the volume of the (anti)cluster droplets max K_A as $|\langle L\rangle| \simeq \max K_{acl} - \max K_{cl}$. Then at $\beta < \beta_c$ one finds that max $K_{acl} =$ max K_{cl} and, hence, $|\langle L\rangle| = 0$. For $\beta \geq \beta_c$ one finds that max $K_{acl} >$ max K_{cl} and the mean value of Polyakov loop is non zero. The mean size of these droplets max K_A defined as

$$\max K_A = \sum_{k=1} k^{1+\tau} n_A(k) \Big/ \sum_{k=1} k^{\tau} n_A(k)\,, \tag{7}$$

is shown in Fig. (6) as a function of β.

Similarly to the reduced surface tension coefficient, the behavior of max K_A for $\beta > \beta_c$ is parameterized as

$$\max K_A(\beta) = \max K_A(\beta_c) \pm a_A(\beta - \beta_c)^{b_A}, \tag{8}$$

where the signs "+" and "-" correspond to A=acl and A=cl, respectively. Here b_A is the critical exponent and a_A is the normalization constant. The found values of these parameters are given in Table 1. It is remarkable that the exponents b_A are close to the ones of the 3-dimensional Ising model $\beta_{Ising} = 0.3265 \pm 0.0001$ [13] and of simple liquids $\beta_{liquids} = 0.335 \pm 0.015$ [14], which reflects the

fact that SU(2) gluodynamics possibly belongs to the same universality class as these systems. Eqs. (6) and (8) allows us to establish a direct relation between the reduced surface tension coefficient and the mean droplet size.

Table 1. The fit parameters according to Eq. (6) for surface tension and Eq. (8) for mean droplet size.

		surface tension			average maximal cluster		
L_{cut}	Type	d_A	B_A	χ^2/dof	a_A	b_A	χ^2/dof
0.1	Cl	0.485(14)	0.2920(12)	1.43 /4	3056(246)	0.2964(284)	16.32 /4
0.1	aCl	2.059(28)	0.4129(77)	1.68/4	2129(160)	0.3315(269)	8.94/4
0.2	Cl	0.2796(118)	0.2891(16)	1.11/4	4953(443)	0.3359(289)	12.3/3
0.2	aCl	1.344(33)	0.4483(21)	0.66/2	2462(88)	0.3750(129)	2.068/4

6 Conclusions

In the present work we report the results of our study of the properties of Polyakov loop geometrical clusters in SU(2) gluodynamics. Based on the analysis of the (anti)cluster size distributions we argue that the deconfinement PT in this pure gauge theory is a special kind of the liquid-gas PT. Introduction of the liquid-gas framework to SU(2) gluodynamics is physically justified due to prominent separation of the "liquid" and "gas" branches of the (anti)cluster size distributions. Unlike to the ordinary liquids, the cluster and anticluster liquids behave differently in the region of broken Z(2) global symmetry. The cluster liquid droplet evaporates above PT whereas the anticluster liquid droplet experiences a condensation of the accompanying gas of anticlusters. A quantitative analysis of the (anti)cluster size distribution is performed using the LDF. Its successful application is one of the most important results of the present work, which also supports the liquid-gas nature of the deconfinement PT in SU(2) gluodynamics. This approach allowed us to determine the dependences of the reduced chemical potential μ_A and the reduced surface tension coefficient σ_A on the lattice parameter β. While in symmetric phase these quantities are identical for clusters of both types, their behavior is drastically different in the deconfined phase. A determination of the Fisher topological constant $\tau = 1.806 \pm 0.008$ with high precision is another important result of this study. The found value of τ is the same both for clusters and for anticlusters and it agrees with the prediction of an exactly solvable model of the nuclear liquid-gas PT [11], while it contradicts to the FDM [8]. Our analysis of the reduced surface tension coefficient and the mean size of the largest (anti)cluster allowed us to conclude that these quantities can serve as an order parameters of the deconfinement PT in SU(2) gluodynamics.

Acknowledgments

The authors thank D. B. Blaschke, O. A. Borisenko, V. Chelnokov, Ch. Gattringer, D. H. Rischke, L. M. Satarov, H. Satz and E. Shuryak for the fruitful discussions and valuable comments. The present work was supported in part by the program "On perspective fundamental research in high-energy and nuclear physics" launched by the Section of Nuclear Physics of National Academy of Sciences of Ukraine and by the NAS of Ukraine grant of GRID simulations for high energy physics.

References

[1] L. G. Yaffe and B. Svetitsky, Phys. Rev. D **26**, 963, 1982.
[2] L. G. Yaffe, and B. Svetitsky, Nucl. Phys. B **210**, 423, 1982.

[3] S. Fortunato and H. Satz, Phys. Lett. B **475**, 311, 2000.
[4] S. Fortunato et. al., Phys. Lett. B **502**, 321, 2001.
[5] C. Gattringer, Phys. Lett. B **690**, 179, 2010.
[6] C. Gattringer and A. Schmidt, JHEP **1101**, 051, 2011.
[7] M. E. Fisher, Physics **3**, 255, 1967.
[8] M. E. Fisher, Rep. Prog. Phys. **30**, 615, 1969.
[9] A. I. Ivanytskyi et al., arXive:1606.04710 [hep-lat].
[10] J. Fingberg, U. Heller and F. Karsch, Nucl. Phys. B **392**, 493, 1993.
[11] V.Sagun, A.Ivanytskyi, K.Bugaev and I.Mishustin, Nucl.Phys. A **924**, 24, 2014.
[12] L. Moretto et al., Phys. Rev. Lett. **94**, 202701, 2005.
[13] M. Campostrini, A. Pelissetto, P. Rossi and E. Vicari, Phys. Rev. E **65**, 066127, 2002.
[14] K. Huang, *Statistical Mechanics* (Wiley, New York, 1987).